# NUCLEAR- AND ASTROPHYSICAL INTERPRETATION OF THE CA-TI-CR ISOTOPIC ANOMALIES IN THE INCLUSION EK 1-4-1 OF THE ALLENDE-METEORITE

W. BÖHMER[1], K.-L. KRATZ[1], B. PFEIFFER[1]
C. FREIBURGHAUS[2], T. RAUSCHER[2], F.-K. THIELEMANN[2]

[1] *Institut für Kernchemie, University Mainz, Fritz-Straßmann-Weg 2*
*D-55128 Mainz, Germany*

[2] *Universität Basel, Department für Physik und Astronomie, Klingelbergstraße 82,*
*CH-4056 Basel, Switzerland*

**Abstract**

In the framework of our investigation to explain the nucleosynthetic origin of the correlated Ca-Ti-Cr Isotopic Anomalies in the refractory inclusion EK 1-4-1 of the Allende Meteorite, $\beta$-decay properties and deformation of the nuclear shape as well as neutron capture cross sections of neutron-rich isotopes in the N=28 region have been determined. These nuclear data are important input parameters for dynamic astrophysical calculations in a complete reaction network. As astrophysical scenario a high entropy bubble at the outer core of a type II supernova was assumed. It will be outlined that at certain entropies between 1 and 200 $k_B$/Baryon the observed Ca-Ti-Cr Anomalies can be reproduced simultaneously.

## 1 Introduction

The progress in understanding nucleosynthesis is closely combined with the knowledge of physical properties of nuclei. In this context, both, the extraction of nuclear data, observable in experiments and by the use of self-consistent models is aspired. In particular, if energy levels, spin and parity as well as deformation are known, reaction-rates and $\beta$-decay properties can be determined. For r-process like scenarios neutron separation energies ($S_n$), half-lives ($T_{1/2}$) and the probability of $\beta$-delayed neutron emission ($P_n$) of nuclei far from stability are of intereset mainly for three reasons. (i) By investigation of these nuclear structure properties the behaviour of nuclei with increasing neutron number can be studied. With the $T_{1/2}$- and $P_n$-values, the nuclear shape can be determined at least for light nuclei due to the fact that only a few energy levels have a significant influence on the global $\beta$-decay properties. These parameters can be considered in the theoretical description and improve the predictive power of the models. (ii) Approximately half of the stable isotopes above the iron group elements are created in the r-process. During this neutron capture process the vicinity of the closed neutron shells $N$=28, 50, 82 and 126 will be reached quickly. In order to reproduce the observed solar r-process abundances the investigation of $\beta$-decays after and during neutron-capture as well as the discovery of the branching-points and the so called *turning-points* are important. Branching appears at nuclei where the number of further neutron captures is of the same order as the number of $\beta$-decays ($T_{1/2}(\mathrm{n}) \simeq T_{1/2}(\beta)$). Whether a nucleus has such branching-points depends i. a. on the neutron-separation energy ($S_n$). With the measurement of the global nuclear physics parameters the models can be improved as mentioned above. That leads to reliable predictions concerning deformation and $S_n$-values. Turning-points appear at nuclei with a relativly small neutron capture cross section so that $\beta$-decays dominate further neutron-captures ($T_{1/2}(\mathrm{n}) > T_{1/2}(\beta)$). If the branching- and turning-points are known, the nucleosynthetic-path can be determined more exactly. This admits the conclusions of temperature ($T_9$) and neutron-density ($n_n$) of mass-rich stars where the r-process takes place. Thus the number of possible astrophysical scenarios can be limited. (iii) The understanding of nucleosynthesis in our solar-system is closely combined with the clarification of the origin of isotopic composition in meteorites. In the context of this investigation, isotopic compositions which differ from those of the remaining solar system, the so called isotopic anomalies, were found in Ca-Al rich inclusions of primitive meteorites. In such high temperature condensates of the stardust, inhomogenities can be covered which derive probably from one single nucleosynthetic event. These condensates are the best source of information of protosolar element- and isotopic-compositions [1]. The explanation of these anomalies can also be received if the nuclear properties of its instable progenitors are understood. It could be shown already in earlier investigations that the $\beta$-delayed neutron emission of neutron rich progenitor isotopes influence directly the isotopic abundance of $^{48}$Ca/$^{46}$Ca in the refractory inclusion EK 1-4-1 of the Allende-Meteorite [2].

## 2 The Experiment

In order to delimit the uncertainties in nuclear-structure properties, already mentioned above, we performed an experiment at the Grand Accelerateur National d'Ion Lourds (GANIL) in Cean, France. In this experiment the gross nuclear properties $T_{1/2}$ and $P_n$ of the neutron-rich isotopes $^{43}$P, $^{42}$S, $^{44}$S, $^{45}$S, $^{44}$Cl, $^{45}$Cl, $^{46}$Cl and $^{47}$Ar could be measured. The isotopes were produced by the methode of projectile fragmentation. The separation of the fragments was done by the use of LISE3 spectrometer. Our detector-system was a $\beta$-telescope consisting of three silicon detectors with a thickness of 300 $\mu$m for the first and the second detector and 5500 $\mu$m for the third one. This $\beta$-telescope was placed at the end of the beam tube. It was surrounded by the neutron detector consisting of a polyethylen moderator where 60 $^3$He-tubes were placed in three concentrical rings. The $\beta$-telescope delivered the $\Delta$E1, $\Delta$E2 and the E3 signal. With the complete detector system single $\beta$- and neutron events, and $\beta$-neutron coincidences could be observed. The experimental setup and the identification of the isotopes are described in detail in [3].

In this experiment half-lives and $P_n$-values of the isotopes $^{43}$P, $^{42}$S, $^{44}$S, $^{45}$S, $^{44}$Cl, $^{45}$Cl, $^{46}$Cl and $^{47}$Ar were measured. The half-lives of $^{44}$S, $^{45}$Cl and $^{46}$Cl which were already obtained in an earlier experiment could be confirmed. The experimental results are outlined in Tab. 1.

## 3 Deformations from a QRPA Parameter Study

One of the motivating questions for the parameter study was to get at least a

**Tab. 1** QRPA-calculation of $T_{1/2}$ and $P_n$ with an optimized quadrupole deformation $\varepsilon_2$ of the investigated nuclei. In column 2 the quadrupole deformation is given which leads to the best agreement between the calculated $T_{1/2}$- and $P_n$-values (columns 3 and 4) and the experimentaly observed values (columns 5 and 6).

| Isotop | $\varepsilon_2$ | optimized adjustment | | experimental values | |
|---|---|---|---|---|---|
| | | $T_{1/2}$[ms] | $P_n$[%] | $T_{1/2}$[ms] | $P_n$[%] |
| $^{43}$P | $-0,175$ | 70 | 100,0 | 36±4 | 100±10 |
| $^{42}$S | $-0,300$ | 1300 | 0,9 | 579±46 | <4 |
| | $+0,300$ | 1570 | 0,1 | | |
| $^{44}$S | $+0,325$ | 133 | 15,3 | 123±10 | 18±3 |
| $^{45}$S | $-0,200$ | 83 | 39,8 | 72±5 | 54±6 |
| | $+0,125$ | 90 | 36,7 | | |
| $^{44}$Cl | $-0,250$ | 434 | 1,8 | 438±19 | <8 |
| $^{45}$Cl | $-0,200$ | 392 | 10,4 | 412±39 | 38±5 |
| $^{46}$Cl | $+0,100$ | 204 | 57,9 | 223±37 | 60±9 |
| $^{47}$Ar | $-0,180$ | 705 | 0,1 | 613±197 | <1 |
| | $+0,125$ | 709 | 0,1 | | |

first idea of the nuclear shape of the investigated nuclei. The nuclei examined in this work, contain 15 to 18 protons and 26 to 29 neutrons. In this low mass region the single-particle levels do not have a high density in the Nilsson-diagram. The energy distance is about 1-5 MeV. This leads to the fact that there are only a few Gamow-Teller transitions possible. $T_{1/2}$ and $P_n$ are dominated by one or two strong transitions in the corresponding energy interval. Thus the investigated correlation between the gross $\beta$-decay properties and the nuclear shape of the corresponding nuclei is unambiguous at least in the fundamental decision whether the nucleus is spherical or deformed. If heavier nuclei are examined this is certainly not the case due to the high level-density (approx. 10 levels per MeV).

In the detailed parameter study $T_{1/2}$ and $P_n$ were calculated as a function of the quadrupole deformation $\varepsilon_2$. The $\varepsilon_2$-values were varied from -0.35 to 0.35. Starting from the FRDM-model prediction $^{44}$S should be spherical. This would lead to the gross $\beta$-decay properties $T_{1/2} = 1.12$ s and $P_n = 100\%$. However, since the first GANIL experiment in 1991 we know: $T_{1/2} = (123 \pm 10)$ ms, $P_n = (18 \pm 3)\%$ [4]. The discrepancy concerning the half-live is a factor of 10, the $P_n$-value is a factor of 5 less than in the prediction. A spherical shape of the nucleus $^{44}$S can be excluded. Good agreement with the experimentally observed values is reached if a prolate deformation of $\varepsilon_2 = 0.325$ is assumed: $T_{1/2}$= 133 ms, $P_n$= 15.3%. Similar results are obtained for other investigated nuclei. Tab. 1 summarizes the quadrupole deformation which leads to the best agreement with the experimentally observed values. For $^{42}$S, $^{45}$S and $^{47}$Ar it can not be determined whether the shape is prolate or oblate deformed. For $^{42}$S the absolute value is the same for both possible deformations, $|\varepsilon_2| = 0.300$. Meanwhile an experiment at Michigan State University (MSU) was performed where the B(E2)-values of $^{36-44}$S were measured via Coulomb-exitation [7]. The absolute value of the quadrupole deformation can be determined directly from the B(E2)-values. The deformation values obtained from the parameter study for $^{42}$S and $^{44}$S are in excellent agreement with the experimentally observed ones. Although in the experiment no information of the sign is given. For the calculation of the neutron-capture cross sections only the absolute deformation value is needed due to the equally increasing level-density.

For $^{45}$S we get a prolate and an oblate value which both reproduces the experimental results. The values differ a bit. The prolate value is in agreement with the RMF-prediction [5]. The QRPA-calculation of $^{47}$Ar reaches good agreement with the experimental values for $\varepsilon_2$=-0.180 and +0.125.

## 4 Network calculations

Important input data in the calculation of nucleosynthesis are neutron-capture cross section ($\sigma_n$). Typical astrophysical neutron energies favor two reaction mechanisms [6]: (i) capture reactions where a *compound nucleus, CN* is created. Cross sections will be calculated by the use of the statistical model of Hauser-Feshbach; and (ii) reactions where a neutron is directly captured into bound states (*direct capture, DC*). The DC-mechanism can dominate the neutron-capture for nuclei with low lying level density in the vicinity of the neutron separation energy. This is especially the case for even-even nuclei because here the level density is lower compared to in nuclei with one or two unpaired nucleons. Thus in addition to the CN-cross sections the DC-contribution of the even-even nuclei from $^{40}$S to $^{74}$Fe were calculated [6].

Nucleosynthesis in the late phase of a massiv star is dominated by neutron capture reactions. The process paths as well as the development of the star can be calculated by computers nowadays. The reliability of such calculations depends on nuclear properties of the involved isotopes. Thus, in our calculations of nucleosynthesis all nuclear input data such as energy-levels, neutron-separation energies, spin and parity, nuclear shape, neutron-capture cross sections and decay-properties were taken into account. If available experimental data were used; if not, the input data were calculated by the use of *internally consistent* models. In this work we tried to find a process which synthesises much $^{48}$Ca, $^{50}$Ti and $^{54}$Cr. The deduced stellar parameters, especially neutron density ($\rho_n$), radiation-entropy ($S \propto T_9^3/\rho$) and time scale of the process ($\tau$), point out the possible astrophysical scenarios.

In the late phase of massiv stars rapid neutron capture can occur. But first of all, due to the high temperatures $T_9 \geq 3$, reactions with charged particles such as (p,$\gamma$), (p,n), ($\alpha$,n) and ($\alpha$,$\gamma$), the reverse reactions, $\beta^+$-decay and electron capture take place. Due to that the computer-code is organized in two steps. The network which calculates the reactions with charged particles in the so called *$\alpha$-process* is developed by F.-K. Thielemann and extends from H to Pd (Z=46). On the neutron-rich side all nuclei up to the neutron-drip line are included. On the proton-rich side the first three isotopes beginning from $\beta$-stability are taken into account. After the calculations in the $\alpha$-process, further calculations will be performed with the r-process code from C. Freiburghaus. This makes sense if there exits one or more free neutrons per seed-nuclei ($Y_n/Y_{seed} \leq 1$). A detailed description of the physical processes and the requested system of equations is given in [8]. The r-process calculations are fully dynamical and do not make use of the (n,$\gamma$)-($\gamma$,n) equilibrium as former calculations did.

### 4.1 Reproduction of the Isotopic-Ratios

In this work the network-calculations were applied to find out if the observed isotopic anomalies can be reproduced. During the process the stellar temperature varies from $T_9 \simeq 9$ to 2.6. As electron abundances $Y_e =< Z/A >$ in the astrophysical scenario the values 0.42, 0.45 and 0.48 were choosen. In Fig. 1 the abundance ratios for $^{48}$Ca/$^{46}$Ca, $^{48}$Ca/$^{50}$Ti and $^{48}$Ca/$^{54}$Cr at $Y_e = 0.42$ are displayed. The entropy is varied from $S = 3$ to 300 k$_B$/Baryon. The dashed lines represent the values observed in EK 1-4-1.

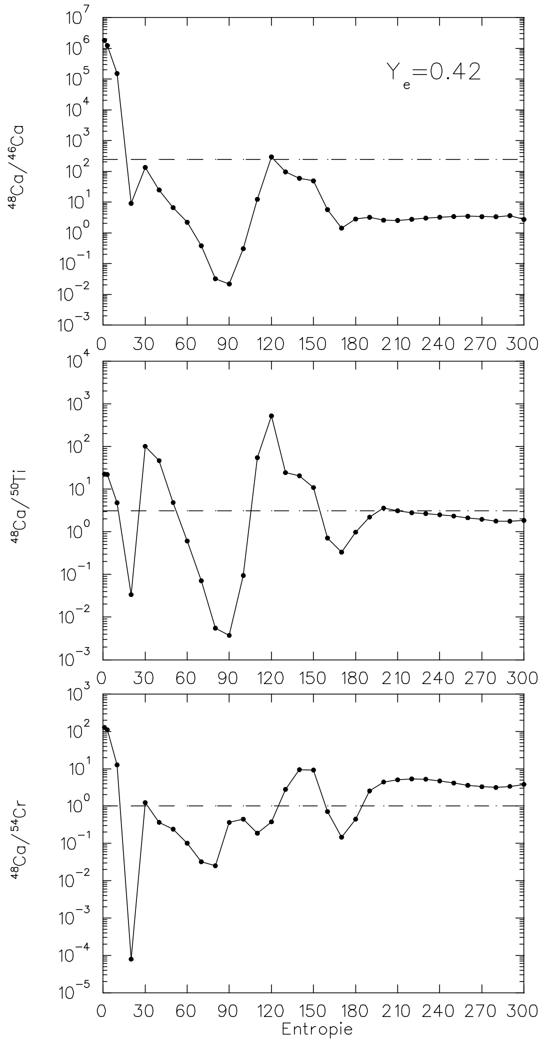


Fig. 1 Calculated isotopic-ratios dependent on entropy. The $Y_e$-value equals 0.42.

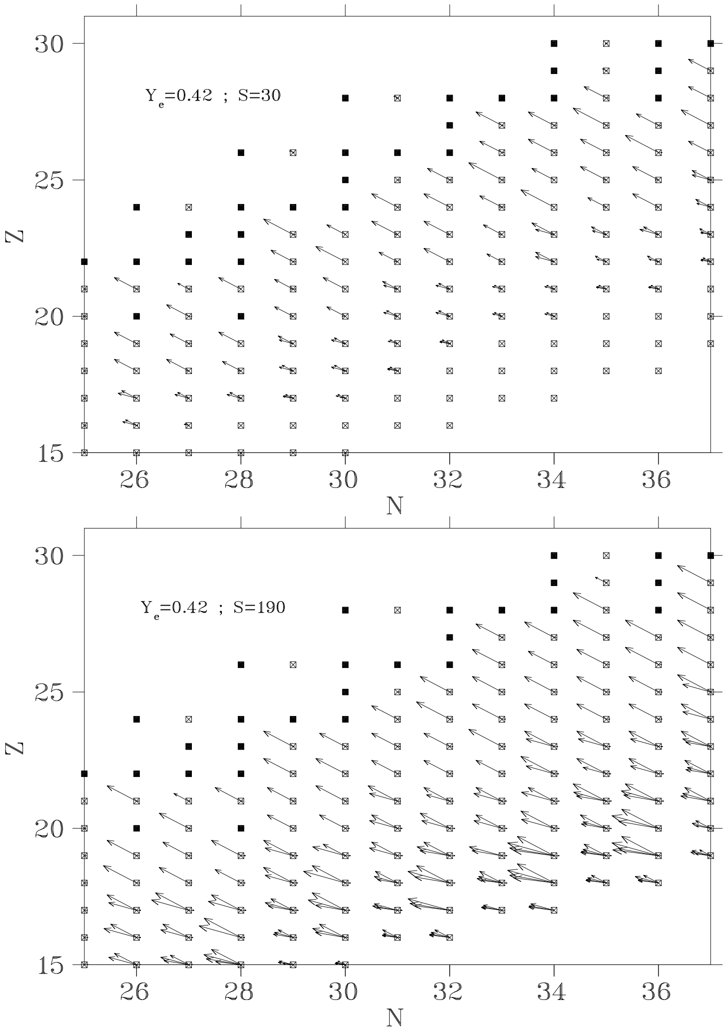


Fig. 2 Flow-charts obtained from the r-process calculations. Shown is the status after neutron-capture just before the different decay-modes start.

The isotopes $^{48}$Ca, $^{50}$Ti and $^{54}$Cr are the most neutron-rich ones observed in the corresponding isotopic chain. Plotted are the ratios $^{48}$Ca/$^{46}$Ca, $^{48}$Ca/$^{50}$Ti and $^{48}$Ca/$^{54}$Cr, because they represent the most sensitive test for the reproduction of the anomalies. In solar matter normaly less neutron-rich isotopes of each isotopic chain were mostly produced due to the homogenization. A simultaneous reproduction of the observed abundance ratios is obtained at the entropies $S = 30$, 130 and 190 k$_B$/Baryon.

In Fig. 2 the flow charts with the electron abundance $Y_e = 0.42$ and two different entropies $S = 30$ (upper part) and $S = 190$ (lower part) are shown. The figures are a snapshot where the most neutron-rich isotopes in each chain are reached just before the different decay-modes start ($\beta$-decay, $\beta$-delate emission of one, two or more neutrons). In the plots this is marked with the corresponding arrows. Fig. 2 shows that a higher entropy leads to more neutron-rich isotopes. This makes sense, because at high entropies the alpha-rich freeze-out leaves more neutrons, which can be captured.

### 4.2 Possible Astrophysical Scenario

As astrophysical scenario for this type of nucleosynthesis a type II supernova can be considered. At the entropy $S \simeq 30$ k$_B$/Baryon the isotopes are synthesized in a process of $\alpha$-rich freeze-out. $^{48}$Ca is built directly without significant neutron captures. The observed anomalies are also obtained with entropies of $S \simeq 150$ and 190 k$_B$/Baryon. In this case $^{48}$Ca is generated by $\beta$-decay of $^{48}$Ar. The astrophysical location in these cases is presumably the outer core of a type II supernova. Typical values for the produced masses with $S = 150$ k$_B$/Baryon are $1 \times 10^{-10}$ M$_\odot$ for $^{46}$Ca, $4 \times 10^{-8}$ M$_\odot$ for $^{48}$Ca, $2 \times 10^{-9}$ M$_\odot$ for $^{50}$Ti and $3 \times 10^{-8}$ M$_\odot$ for $^{54}$Cr. This is about 2 to 3 orders of magnitude less than in a type Ia supernova. In addition type II supernovae events are approximately 10 times more seldom than type Ia supernovae. All together the contribution of produced and ejected matter on type II supernovae is a factor $10^3$ till $10^4$ less than via type Ia supernova scenarios and therefore not sufficient to generate the solar $^{48}$Ca, $^{50}$Ti and $^{54}$Cr. The majority of the solar matter is built in SN Ia. This is in agreement with [9]. However, the amount of matter ejected by type II supernovae is enough to explain the observations in EK 1-4-1. First evidence that the outer core of a type II supernova can be considered as astrophysical scenario, is already mentioned in [10].

## 5 Summary

The parameter study showed clearly that the experimentally observed $T_{1/2}$- and $P_n$-values can only be reproduced when significant quadrupole-deformation is assumed. The nuclear shape and therefore ist locations of the single-particle levels are crucial nuclear physics input-parameters for r-process calculations. Due to this, it is a challenge to observe quadrupole deformation via Coulomb excitation. First experiments showed already that this is nowadays possible. Further the flow chart of each nucleosynthesis calculation gives information about the isotopes involved. The comparison with the observed abundance pattern leads to isotopes whose decay properties are especially worth to be investigated by experimentalists. The better the process paths can be determined owing to the nuclear physics parameters the more exact statements of stellar temperature, neutron density and entropy can be made. A detailed investigation of these correlations and therefore of the chemical evolution in SN Ia and SN II is of interest.

## 6 Acknowledgement

The QRPA-calculations were performed in collaboration with P. Möller. Financial support from the German DFG are gratefully acknowledged.

## References

[1] U. Ott, Nature **364** (1993) 25

[2] W. Ziegert, PhD-Thesis, University of Mainz, 1985

[3] W. Böhmer, PhD-Thesis, University of Mainz, 1996

[4] O. Sorlin et al., Phys. Rev. C47 (1993) 2941

[5] T. R. Werner et al., Phys. Lett. B333 (1994) 303

[6] T. Rauscher et al., Proceedings ENAM, Arles (1995)

[7] T. Glasmacher et al., Phys. Lett. B 395 (1997) 163

[8] C. Freiburghaus, Diploma-Thesis, University Basel, 1995

[9] B. S. Meyer et al., Ap. J. 462 (1995) 825

[10] K.-L. Kratz et al., Physikalische Blätter 51 (1995) 183